Heliyon 9 (2023) e21220

Contents lists available at ScienceDirect

Heliyon

journal homepage: www.cell.com/heliyon

Salidroside attenuates atrial fibrosis and atrial fibrillation vulnerability induced by angiotensin-II through inhibition of LOXL2-TGF-β1-Smad2/3 pathway

Zhen Hai [a,1], Yingbiao Wu [b,1], Zhongping Ning [b,*]

[a] Department of Cardiology, Shanghai University of Traditional Chinese Medicine, 1200 Cailun Road Zhangjiang Hi-Tech Park, Pudong New Area, Shanghai, 201203, China

[b] Department of Cardiology, Shanghai Pudong New Area Zhoupu Hospital (Zhoupu Hospital affiliated to Shanghai Medical College of Health), No.1500 Zhouyuan Road, Pudong New District, Shanghai 201318, China

ARTICLE INFO

Keywords:
Salidroside
Atrial fibrillation
Atrial fibrosis
Angiotensin II
Lysyl oxidase-like 2

ABSTRACT

Aims and objectives: Salidroside (SAL), an active component isolated from the Chinese plant Rose Rhodiola, has anti-inflammatory, antioxidant, anti-cancer, neuroprotective, and renal protective properties. Atrial fibrosis developed due to angiotensin II (Ang II) plays a crucial function in developing atrial fibrillation (AF). This research investigates the involvement of SAL in AF, its vulnerability to AF, and Ang II-induced inflammatory atrial fibrosis.

Methods: Ang II (2 mg/kg/day) was infused underneath the skin into male C57BL/6 mice (8–10 weeks old, n = 40) for four weeks to create the AF model. SAL (50 mg/kg/day) was given intraperitoneally once per day for 28 days. Analyses of morphology, histology, and biochemical were carried out. Transesophageal burst pacing was used in vivo to induce AF.

Results: Ang II injection increased mice's heart rate and systolic blood pressure (SBP), whereas SAL treatment was significantly reduced. Ang II infusion increased left atrial diameter (LAD) in mice, which was attenuated after SAL treatment. SAL alone did not affect AF inducibility, but SAL therapy markedly decreased Ang II-induced AF inducibility. Additionally, the expression levels of interleukin-1 beta (IL-1β), interleukin-6 (IL-6) and tumor necrosis factor-alpha (TNF-α) were inhibited with SAL therapy in mice. Compared to the Ang II group, Ang II infusion raised malondialdehyde (MDA) levels and reduced superoxide dismutase (SOD) and catalase (CAT) activity, but SAL therapy altered all of these effects. SAL treatment significantly reduced LOXL2, TGF-β1, *p*-Smad2 and *p*-Smad3 protein expression than the Ang II group mice.

Conclusion: SAL inhibits atrial fibrosis and potentially attenuates increased susceptibility to AF by suppressing the LOXL2-TGF-β1-Smad2/3 pathway.

1. Introduction

A cardiac rhythm that is inconsistent and frequently extremely fast is known as atrial fibrillation (AF), which raises the risk of heart failure, stroke, and cardiac morbidity and mortality [1,2]. Atrial fibrosis is the common cause of atrial remodeling, which is crucial to

* Corresponding author.
E-mail address: ningzpsh@163.com (Z. Ning).
[1] Contributed equally.

https://doi.org/10.1016/j.heliyon.2023.e21220
Received 17 March 2023; Received in revised form 16 September 2023; Accepted 18 October 2023
Available online 20 October 2023

the pathogenic mechanism of AF [3,4]. As a result, reducing atrial fibrosis may be a practical approach for preventing the development and progression of AF.

TGF-β1, or transforming growth factor-beta 1, is a polypeptide cytokine of the transforming growth factor-beta superfamily. TGF-β1 interacts with its type I and II receptors, promoting Smad protein 2, 3, and 4 inactivation prior to the Smad complex translocate into the nucleus and activating the phosphorylation reaction while suppressing the profibrotic proteins collagen and connective tissue growth factor production [1,5]. Several investigations have found that angiotensin II (Ang II) increases TGF-β1 and collagen production both in vitro and in vivo. Ang II also functions in atrial fibrosis and AF by regulating TGF-β1 [6–8]. This evidence suggests that Ang II-infused atrial fibrosis could be reduced via deactivating the TGF-β1/Smads pathway.

Lysyl oxidase-like 2 (LOXL2) belongs to the LOX family. According to a prior investigation, LOXL2 is involved in the onset and development of fibrosis-associated diseases via the formation of epithelial-mesenchymal transition (EMT) and extracellular matrix [9]. In matrix remodeling and fibrogenesis, LOXL2 is crucial [10]. According to a recent study, LOXL2 contributes to cardiac fibrosis in heart failure [11]. In the cardiac interstitium of diseased human hearts, LOXL2 is elevated, according to a different study. The levels of LOXL2 were linked to collagen crosslinking and heart dysfunction. Additionally, a previous study demonstrated that serum in heart failure (HF) patients were LOXL2 enriched, which showed that LOXL2 might have a pathogenic role in atrial fibrosis and HF [12].

Rhodiola is a plant that grows in Asia's western, northern, and subarctic areas and is widely used in traditional Chinese medicine. It belongs to the Crassulaceae subfamily of the Rosaceae [13]. One of the active components of Rhodiola, a tyrosol glycoside known as salidroside (SAL), has been reported to have depressive and anxiety-reducing characteristics [14]. SAL has currently gained more attention due to its various pharmacological properties, including antioxidant, anti-inflammatory, cancer prevention, and protective effects on neurons [15–17]. In mice induced with LPS or paraquat, SAL has been found to lessen acute lung damage [18]. Additionally, SAL attenuates sepsis and acute lung injury in LPS-induced mice [19,20]. However, the mechanism and impact of SAL on Ang II-infused atrial fibrosis and AF are unknown. For this, our study aims to examine and deliver comprehensive information on the possible function of SAL in angiotensin II-infused atrial fibrosis and AF and evaluate the underlying mechanism.

2. Materials and methods

2.1. Animals treatment, grouping and drug administration

The AF model was established using C57BL/6 mice (male, 8–10 weeks, n = 40) administered beneath the layers of the skin with saline or Ang II (2.0 mg/kg/day) employing osmotic mini-pumps for 28 days. The salidroside (SAL, 50 mg/kg/day, HY-N0109, MedChemExpress) or the same volume of saline was injected intraperitoneally once per day for 28 days, with the first injection one day before the beginning of Ang II treatment. The systolic blood pressure (SBP) was assessed by a tail-cuff system (Softron BP98A; Softron Tokyo, Japan) on day 28 before the electrocardiogram. This entire research was approved by the Animal Care and Use Committee of Shanghai Pudong Zhoupu Hospital and confirmed by the Guide for the Care and Use of Laboratory Animals (NIH Publication No. 85-23, revised 1996).

Four groups of mice were assigned in this study: (A) The Control group (n = 8) were treated with saline by intraperitoneal injection and infused with saline. (B) The SAL group (n = 8) were injected with SAL (50 mg/kg/day) by intraperitoneal injection and infused with saline. (C) The Ang II group (n = 8) were administered with saline intraperitoneal injection and Ang II (2.0 mg/kg/day)-induced. (D) The Ang II + SAL group (n = 8) were administered with SAL (50 mg/kg/day) by intraperitoneal injection and Ang II (2.0 mg/kg/day)-induced. The Ethics Committee of Shanghai Pudong New Area Zhoupu Hospital (Zhoupu Hospital affiliated with Shanghai Medical College of Health) approved (2023XM002) the study. By the 1964 Helsinki Declaration, the authors anticipated all conventional protocols. All procedures used in this investigation followed ARRIVE recommendations.

2.2. Arrhythmia inducibility and duration

The mice were anaesthetized after 28 days of therapy with an intraperitoneal injection of 1 % pentobarbital sodium. After the Ang II infusion was completed through the jugular vein, an 8-electrode catheter (Japan Lifeline, Tokyo, Japan) was introduced and progressed to the coronary atrium and ventricular. The AF inducibility was assessed using a computer-based data collecting system (MadLab-4C/501H, ZS Dichuang Co., Ltd., Beijing, China) and a 2-s pulse employing a computerized pacemaker. The following settings were chosen: voltage (20 V), current (4 mA), and wave width (6 ms). A fast, uneven atrial rhythm with inconsistent R–R intervals of 1 s is characterized as AF. The period between the end of bursting pacing and the first P-wave recorded following the fast, inconsistent cardiac rhythm was designated as the duration of AF [8].

2.3. Echocardiography

Two-dimensional M-mode echocardiography was employed to record cardiac structural and functional changes. After mice were anaesthetized with inhalational isoflurane, echocardiography (Vevo 3100; VisualSonics Inc., Toronto, Ontario, Canada) was performed by a blinded animal cardiologist to the experimental grouping. Left atrial diameter (LAD), left ventricular end-diastolic posterior wall thickness (LVPWth), and left ventricular ejection fraction (LVEF) were obtained, respectively [21].

2.4. Sample collection

The atrial tissue was collected after mice were anaesthetized with 1 % pentobarbital sodium. For RT-qPCR and Western blot analysis, some tissue was snap-frozen in liquid nitrogen, while others were fixed in 4 % paraformaldehyde for histopathological examinations.

2.5. Tissue histology and immunohistochemistry

After being treated with 4 % paraformaldehyde, atrial tissue was fixed in paraffin and sliced into 5 μm serial slices. The tissues were cleaned of paraffin in xylene, rehydrated, and inserted into the positively charged slides. The slides were stained with Masson's trichrome or rabbit polyclonal antibodies that react against α-SMA (1:400; ab5694; rabbit polyclonal, Abcam, UK). The secondary antibody was biotinylated by horseradish peroxidase after 20 min at 37 °C. Following cleaning, the slides were counter-stained. Photos were taken using a Nikon X200 magnification lens in Tokyo, Japan, and analyzed with ImageJ (NIH, Bethesda, MD, USA).

2.6. Immunofluorescence

The Immunofluorescence procedure was carried out as previously explained [22]. Mice's atrial tissue was acquired in frozen sections. Following three washes in phosphate-buffered saline (PBS), the sections were stained with TUNEL (C1086, Beyotime) and DHE (S0063, Beyotime) and investigated under an inverted microscope (IX51, Olympus, Japan).

2.7. Oxidative stress

The atrial tissue was homogenised (10 %, w/v) in standard cold saline to assess the MDA (S0131S, Beyotime, Shanghai, China) content, SOD (S0109, Beyotime), and CAT (S0051, Beyotime) endeavours using readily accessible commercial kits. The previously published technique was employed to evaluate the amount of oxidative stress [23].

2.8. RT-qPCR

TRIzol (Invitrogen, Carlsbad, CA, USA) was utilized to extract total RNA. Using the reverse transcription kit, reverse transcription was carried out (TaKaRa, Tokyo, Japan). Using a Light Cycler 480 real-time PCR device, gene expression was discovered (Roche, Indianapolis, IN, USA). The fluorescent quantitative PCR kit's (SYBR Green Mix, Roche Diagnostics, Indianapolis, IN) instructions regarding the reaction conditions were followed. After 45 cycles of 95 °C for 5 s, 60 °C for 10 s, and 72 °C for 10 s, the thermal cycle parameter was 95 °C for 10 s. A final extension was displayed for 5 min at 72 °C. Experiments were repeated three times, and each Ct result was standardized with GAPDH to determine relative expression. The results were examined using the 2-ΔΔCT methodology [24]. The primer oligonucleotide sequences used in this study are presented in Table 1.

2.9. Western blotting

The protein was extracted using RIPA buffer, and the resultant lysates were centrifuged to generate supernatants, and BCA protein assay kit was used to quantify protein quantities. The protein samples (50 μg) were placed onto a 10 % SDS-PAGE gel for electrophoresis, and then protein was moved to a PVDF membrane (Millipore, Bedford, MA). A 5 % skim milk TBS solution occluded the membrane. The membrane was incubated with the following LOXL2 (1:500, ab96233; rabbit polyclonal, Abcam, UK), TGF-β1 (1:500, ab179695, rabbit monoclonal, Abcam), p-Smad2 (1:500, ab188334, rabbit monoclonal, Abcam), P-Smad3 (1:400, ab52903, rabbit monoclonal, Abcam), Smad2 (1:400, ab119907, mouse monoclonal, Abcam), Smad3 (1:400, ab84177, rabbit polyclonal, Abcam), and

Table 1
List of primer sequences used in this study.

Genes	Forward primer (5′–3′)	Reverse primer (5′–3′)
α-SMA	TCCTGACGCTGAAGTATCCGATA	GGCCACACGAAGCTCGTTAT
Collagen I	GCTCCTCTTAGGGGCCACT	CCACGTCTCACCATTGGGG
Collagen III	TCCCCTGGAATCTGTGAATC	TGAGTCGAATTGGGGAGAAT
IL-1β	GAAATGCCACCTTTTGACAGTG	TGGATGCTCTCATCAGGACAG
IL-6	AACCACGGCCTTCCCTACT	CATTTCCACGATTTCCCAGA
TNF-α	CGTCGTAGCAAACCACCAA	GGGCAGCCTTGTCCCTTGA
NOX2	TGGCGATCTCAGCAAAAGGT	ACCTTGGGGCACTTGACAAA
NOX4	ACCAAATGTTGGGCGATTGTG	GATGAGGCTGCAGTTGAGGT
LOXL2	ATGACAGCAGGAGCGTGAGGT	GGTTTAGAGCAGCAGAGAAGGGTAAG
TGF-β1	AGCAACAATTCCTGGCGTTACCTT	CCTGTATTCCGTCTCCTTGGTTCAG
GAPDH	ACTCCACTCACGGCAAATTC	TCTCCATGGTGGTGAAGACA

Abbreviation: α-SMA, α-smooth muscle actin; IL-1β, interleukin-1β; IL-6, interleukin-6; TNF-α, tumor necrosis factor-α; NOX2, NADPH Oxidase 2; LOXL2, lysyl oxidase-like 2; TGF-β1: transforming growth factor-β1; GAPDH: Glyceraldehyde-3-phosphate dehydrogenase.

GAPDH (1:1000, ab9485, rabbit polyclonal, Abcam) antibodies overnight at 4 °C. HRP-conjugated secondary antibodies (1:2000) were used to identify the immunological reactivity of the targeted proteins. By employing ECL (Thermo, Waltham, MA, USA), the protein band was seen, and band density was calculated by the image software (Bio-Rad, Hercules, CA, USA).

2.10. Statistical analysis

The data was represented as the mean ± standard deviation (SD) and was repeated three times. Statistical analyses were carried out using SPSS 20.0 (SPSS, Chicago, IL, USA). The differences between three or more groups were assessed by the one-way ANOVA. To compare the prevalence of AF among four groups, Fisher's exact test was performed. The level of statistical significance was chosen at $P < 0.05$.

3. Results

3.1. Physiological and echocardiographic parameters in mice

After mice were induced with Ang II (2 mg/kg/day) and SAL (50 mg/kg/day) for 28 days, we assessed the potential changes in body weight, heart rate, and systolic blood pressure (SBP). No significant body weight differences were observed among the Control, SAL, Ang II, and Ang II + SAL groups on day 28 (Fig. 1A). Ang II-induced mice exhibited improved heart rate and SBP than saline infusion mice (Control group). SAL potentially reduced the Ang II-induced increase in heart rate and SBP in mice (Fig. 1B and C). Echocardiography on day 28 showed that Ang II injection increased left atrial diameter (LAD) in mice, which was inhibited after SAL treatment (Fig. 1D and E). SAL also attenuated an Ang II-induced enhancement in left ventricular end-diastolic posterior wall thickness (LVPWth) and a reduction in left ventricular ejection fraction (LVEF) than only the Ang II group (Fig. 1F and G).

3.2. SAL reduced Ang II-induced AF

Mice were treated with Ang II or saline, and SAL (50 mg/kg/day) or saline was intraperitoneally injected for 28 days to evaluate the

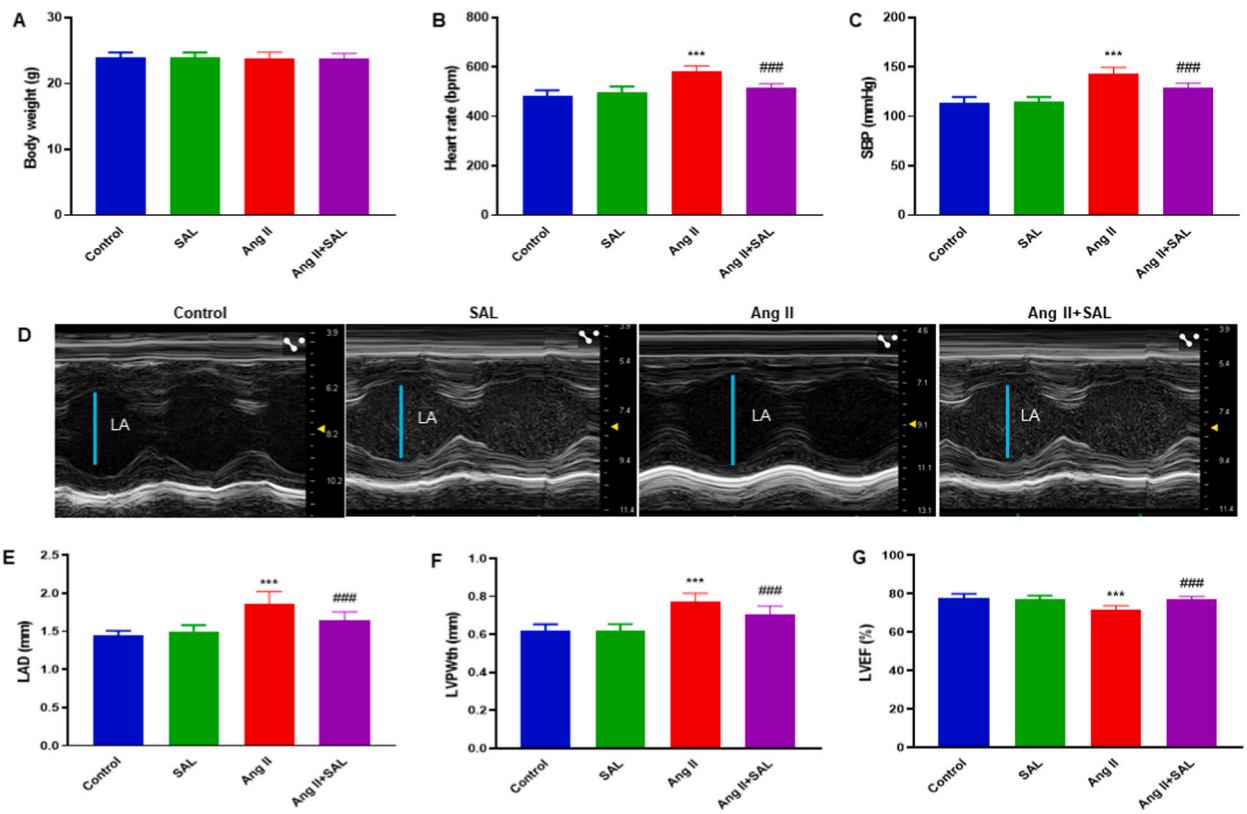

Fig. 1. Physiological and echocardiographic parameters in mice. Serial changes in (A) body weight, (B) heart rate and (C) SBP were monitored in mice after the experimental period of 28 days; (D) Echocardiography of the left atrium (LA) chamber was performed to measure (E) LAD, (F) LVPWth, and (G) LVEF. SBP, systolic blood pressure; LAD, left atrial diameter; LVPWth, left ventricular end-diastolic posterior wall thickness; LVEF left ventricular ejection fraction. Data are presented as mean ± SD. ***P < 0.001 vs. Control group; ###P < 0.001 vs. Ang II group.

effects of SAL on AF susceptibility. Transesophageal rapid atrial pacing was applied to record the electrocardiogram. The results showed that the AF group had typical atrial fibrillation (AF) attacks (Fig. 2A). However, in Ang II or saline-induced mice administered with or without SAL, the inducibility and length of AF were investigated. The AF inducibility was low in mice of the control group but was sharply increased by Ang II infusion. Treatment with SAL substantially decreased the inducibility of AF caused by Ang II. However, we did not observe any impact on the AF inducibility for the only SAL group mice (Fig. 2B). SAL also considerably reduced the total duration of AF in Ang II-induced mice. Still, SAL treatment alone did not significantly change AF duration (Fig. 2C).

3.3. SAL inhibited Ang II-induced atrial fibrosis

The impact of SAL in atrial fibrosis, an indicator of atrial remodeling, was subsequently investigated. Ang II treatment considerably enhanced the atrial fibrotic area. At the same time, SAL therapy potentially reduces the atrial fibrotic area (Fig. 3A). Furthermore, immunohistochemistry revealed that SAL significantly reduced the quantity of α-SMA + myofibroblasts in atrial tissue generated by Ang II (Fig. 3B). RT-qPCR also validated the expression pattern of α-SMA. In addition, the two fibrotic biomarkers expression was evaluated using RT-qPCR. Ang II significantly increased the mRNA levels of collagen I and III in the atrial tissue of mice. Still, these changes were markedly reduced by SAL (Fig. 3C). The treatment of SAL inhibited Ang II-infused IL-1β, IL-6 and TNF-α mRNA expression levels compared with mice with Ang II alone (Fig. 3D).

3.4. SAL suppresses Ang II-infused atrial apoptosis and oxidative stress

TUNEL staining was performed to determine the effect of SAL on atrial tissue apoptosis. TUNEL + cells (green fluorescence) increased significantly after Ang II injection, but this rise was reduced in SAL-treated mice (Fig. 4A). In addition, Ang II administration also enhanced atrial superoxide production (DHE staining), which was attenuated by SAL treatment (Fig. 4B). Key biomarkers of oxidative stress, including MDA, SOD and CAT, were determined in the lysate of atrial tissue. Ang II infusion increased levels of MDA content and decreased SOD and CAT activities compared to the Ang II group, while these changes were all altered by SAL therapy (Fig. 4C, D, 4E). Meanwhile, NOX2 and NOX4 gene expression was determined using RT-qPCR. SAL therapy potentially reduces the

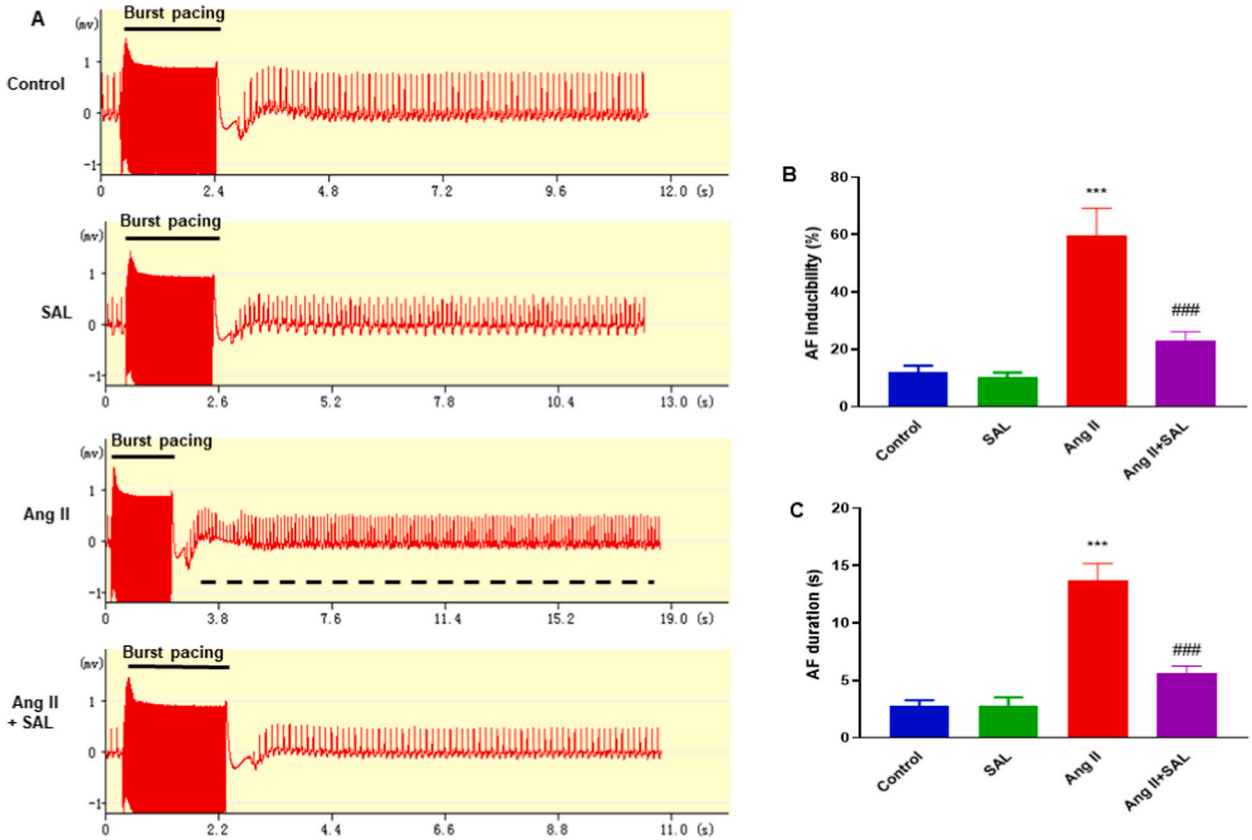

Fig. 2. SAL reduces atrial fibrillation (AF) inducibility and AF duration induced by burst pacing. (A) Representative atrial electrogram recordings. Burst pacing is indicated by solid underlines, whereas dashed underlines indicate AF. (B) Percentage of successful AF inducibility in each group (n = 8). (C) Average AF duration by burst pacing (n = 8 in each group). Data are presented as mean ± SD. ***P < 0.001 vs. Control group; ###P < 0.001 vs. Ang II group.

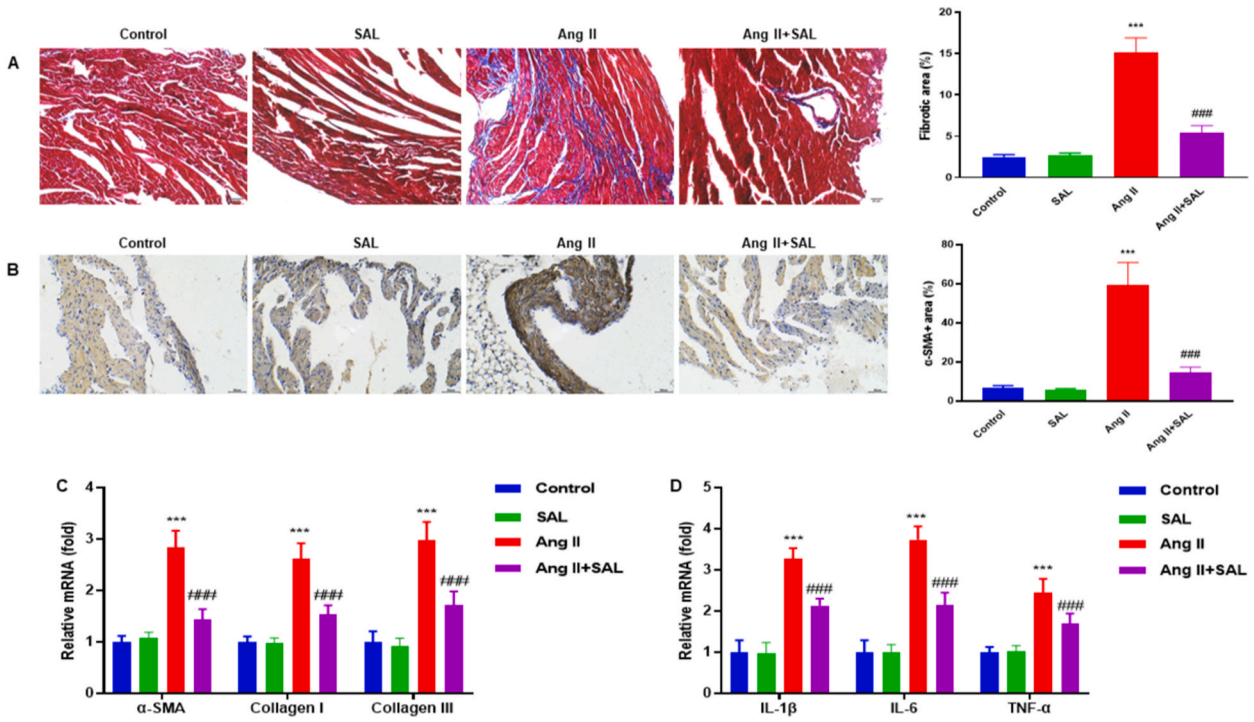

Fig. 3. SAL suppresses Ang II-induced atrial fibrosis. (A) Representative images of Masson trichrome staining for atrial fibrosis. The fibrotic area is quantified to evaluate the extent of atrial fibrosis. (B) Representative images of α-SMA (a marker for myofibroblast differentiation) by immunohistochemistry. The percentage of α-SMA-positive cells is quantified. RT-qPCR was applied to determine the mRNA levels of (C) α-SMA, collagen I and III, and analyzed the mRNA expression levels of inflammatory cytokines, (D) IL-1β, IL-6 and TNF-α in atrial tissues. GAPDH as an internal control. Experiments were run in triplicate. Data are presented as mean ± SD (n = 8 in each group). ***P < 0.001 vs. control group; ###P < 0.001 vs. Ang II group.

NOX2 and NOX4 gene expression than only the Ang II group mice (Fig. 4F).

3.5. SAL inhibited the expressions of proteins of LOXL2 and TGF-β1/Smad pathway

To assess the LOXL2 protein expression level in Ang II-infused mice, we carried out an immunohistochemistry analysis. SAL therapy reduced the protein expression in LOXL2, which was elevated by Ang II injection (Fig. 5A). This changing pattern was also validated at the mRNA level of LOXL2 by RT-qPCR (Fig. 5B). To evaluate the key protein expression level of the TGF-β1/Smad pathway, we performed the Western blot analysis (Fig. 5C). SAL treatment significantly reduced LOXL2, TGF-β1, *p*-Smad2 and *p*-Smad3 protein expression than the Ang II group mice (Fig. 5D and E). However, the total Smad2 and Smad3 protein levels did not change.

4. Discussion

In the current research, we examined the potential function of SAL in Ang II-induced atrial fibrosis and AF. The data demonstrated that SAL potentially decreased the Ang II-infused enhancement in heart rate and SBP in mice. Ang II-induced increased LAD in mice, whereas SAL therapy decreased. SAL suppressed Ang II-induced increasing LVPWth and reducing LVEF than the Ang II group mice. In addition, SAL attenuated Ang II-infused atrial fibrosis and AF, and atrial apoptosis and oxidative stress. Further, SAL reduced the expressions of LOXL2 and TGF-β1/Smad pathway proteins. Thus, the findings imply that SAL could have a possible therapeutic role in atrial fibrosis and AF susceptibility.

Body weight, heart rate, and systolic blood pressure (SBP) were assessed after mice were injected with Ang II and SAL for 28 days. The results did not show any potential body weight changes in the control mice, SAL, Ang II, and Ang II + SAL groups. Ang II group mice showed high heart rates and SBP compared with the control group, but SAL significantly suppressed heart rates and SBP in mice (Fig. 1B and C). Ang II infusion in mice increased left atrial diameter (LAD), which decreased following SAL therapy, according to echocardiography on day 28 (Fig. 1D and E). In contrast to mice treated with Ang II alone, SAL also prevented a rise in LVPWth and a decrease in LVEF that was Ang II-induced (Fig. 1F and G).

An arrhythmia called atrial fibrillation frequently results in life-threatening consequences. Electrical and structural remodeling are two aspects of atrial remodeling connected to AF's development and maintenance. Atrial fibrosis is essential to structural remodeling [24, 25]. In the current study, Ang II-triggered AF inducibility was considerably reduced by SAL treatment, whereas SAL alone did not

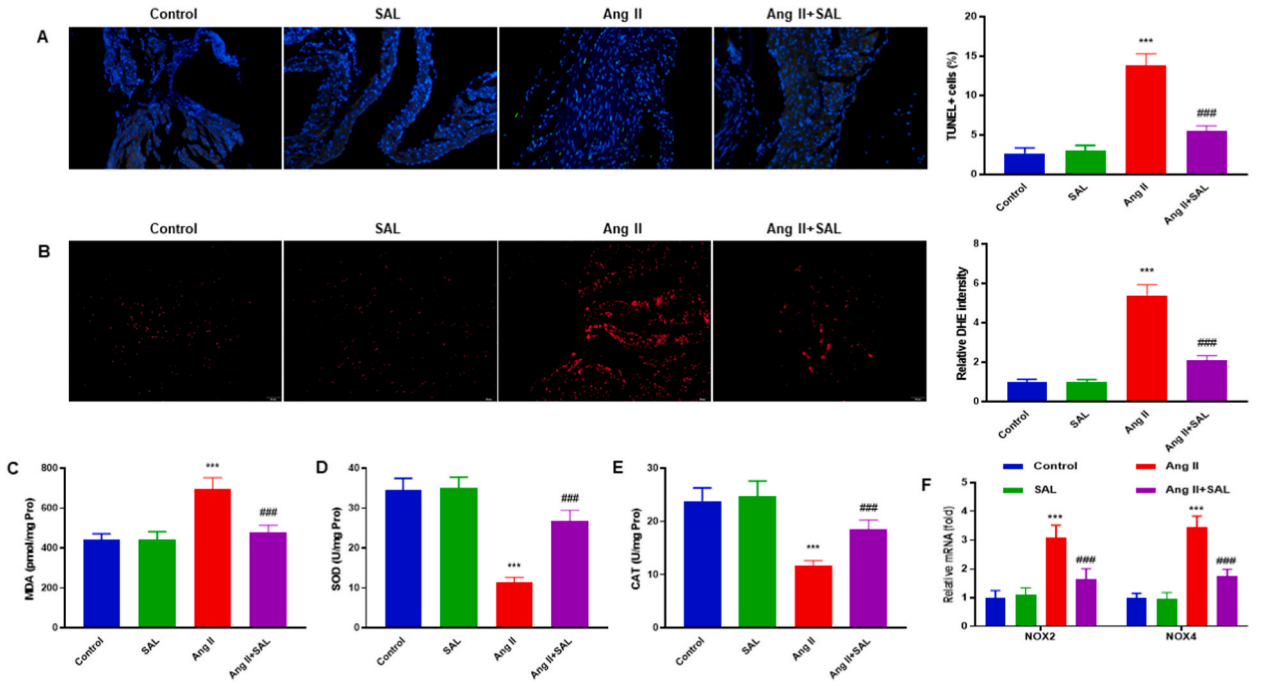

Fig. 4. SAL reduces atrial apoptosis and oxidative stress in mice after Ang II infusion. (A) Representative images of TUNEL staining in the atria. Quantification of TUNEL-positive cells in atrial tissues. (B) Representative images of DHE staining of atrial superoxide and quantification of DHE intensity. The levels of (C) MDA, (D) SOD and (E) CAT in the atrial lysate were quantified. (F) RT-qPCR analyses of the mRNA expression levels of NOX2 and NOX4. GAPDH as an internal control. Experiments were run in triplicate. Data are presented as mean ± SD (n = 8 in each group). ***P < 0.001 vs. control group; ###P < 0.001 vs. Ang II group.

affect AF inducibility in control (Fig. 2B). SAL therapy alone did not result in a significant change in AF length; however, SAL treatment dramatically decreased the overall duration of AF in mice treated with Ang II (Fig. 2C). Therefore, SAL significantly decreased the Ang II-infused AF in mice.

Atrial fibrosis development was significantly mediated by the expression of Ang II, which was elevated in AF patients [1,25]. The earlier investigation showed that Ang II might stimulate TGF-β1 synthesis, secretion, and downstream Smad2 signaling pathways, leading to the Smad2-dependent generation of connective tissue growth factor [26]. As a result, fibroblasts in the myocardium multiply and fibrocytes are encouraged to differentiate into myofibroblasts, ultimately deposing the extracellular matrix (ECM). Our results showed that Ang II greatly enhanced the atrial fibrotic area, but SAL was significantly inhibited (Fig. 3A). Additionally, immunohistochemistry demonstrated that the SAL significantly reduced the levels of α-SMA + myofibroblasts that Ang II-induced increase in atrial tissue (Fig. 3B). Ang II dramatically raised the mRNA levels of collagen I and III in the atrial tissue, whereas SAL was significantly attenuated (Fig. 3C). The SAL treatment attenuated Ang II-induced mRNA expression levels of IL-1β, IL-6 and TNF-α compared with mice with Ang II alone (Fig. 3D). SAL has been shown to inhibit renin-angiotensin system (RAS) activation. However, no study has examined the function of SAL in AF-related RAS system inhibition.

In the present study showed that the administration of SAL decreases Ang II-induced atrial apoptosis and oxidative stress. TUNEL staining showed increasing green fluorescence intensity in Ang II infusion mice, whereas decreasing in the SAL-injected mice (Fig. 4A). DHE staining showed the same trends increasing atrial superoxide formation but attenuating with SAL treatment (Fig. 4B). Oxidative stress biomarkers (MDA, SOD and CAT) determined the lysate of atrial tissue. The levels of MDA content were increased and reduced SOD and CAT levels in Ang II group mice, whereas reversed results were observed with SAL treatment (Fig. 4C, D, 4E). In addition, SAL therapy dramatically decreased the mRNA expression of NOX2 and NOX4 than the Ang II group mice (Fig. 4F). Therefore, SAL significantly attenuates the Ang II-infused atrial apoptosis and oxidative stress in the AF mice model.

The early study showed that heart failure (HF) or atrial fibrillation patients had higher LOXL2 expression [11,12]. The elevated expression of LOXL2 in the ventricular interstitium of HF patients demonstrated that this serum LOXL2 is produced by fibroblasts in the cardiac interstitium [11]. TGF-β1 is essential for developing epithelial-to-mesenchymal transition (EMT) [27]. EMT is produced by TGF-β1, which considerably affects atrial fibrosis and hypertrophy [28,29]. A possible target in the fight against cardiac hypertrophy is the TGF-β1/Smad3 axis, which comprises the downstream protein Smad3. Both cardiac hypertrophy and the transition of fibroblasts into myofibroblasts were inhibited by inhibition of the TGF-β1/Smad3 axis [30]. Moreover, the TGF-β1/Smad3 axis promoted CTGF expression and led to the production of collagen type I in fibroblasts [31]. Because inhibiting LOXL2 reduced the expression of pSmad3 in lung fibroblasts from mice with bleomycin-induced pulmonary fibrosis, this suggests that LOXL2 is upstream of Smad3 [32]. In addition, TGF-β1 mediated endothelium-to-mesenchymal transition (EndMT) activation in endothelial cells was prevented by LOXL2 knockdown [33]. However, this research demonstrated that SAL reduced the effect of Ang II infusion on the expression of the protein in

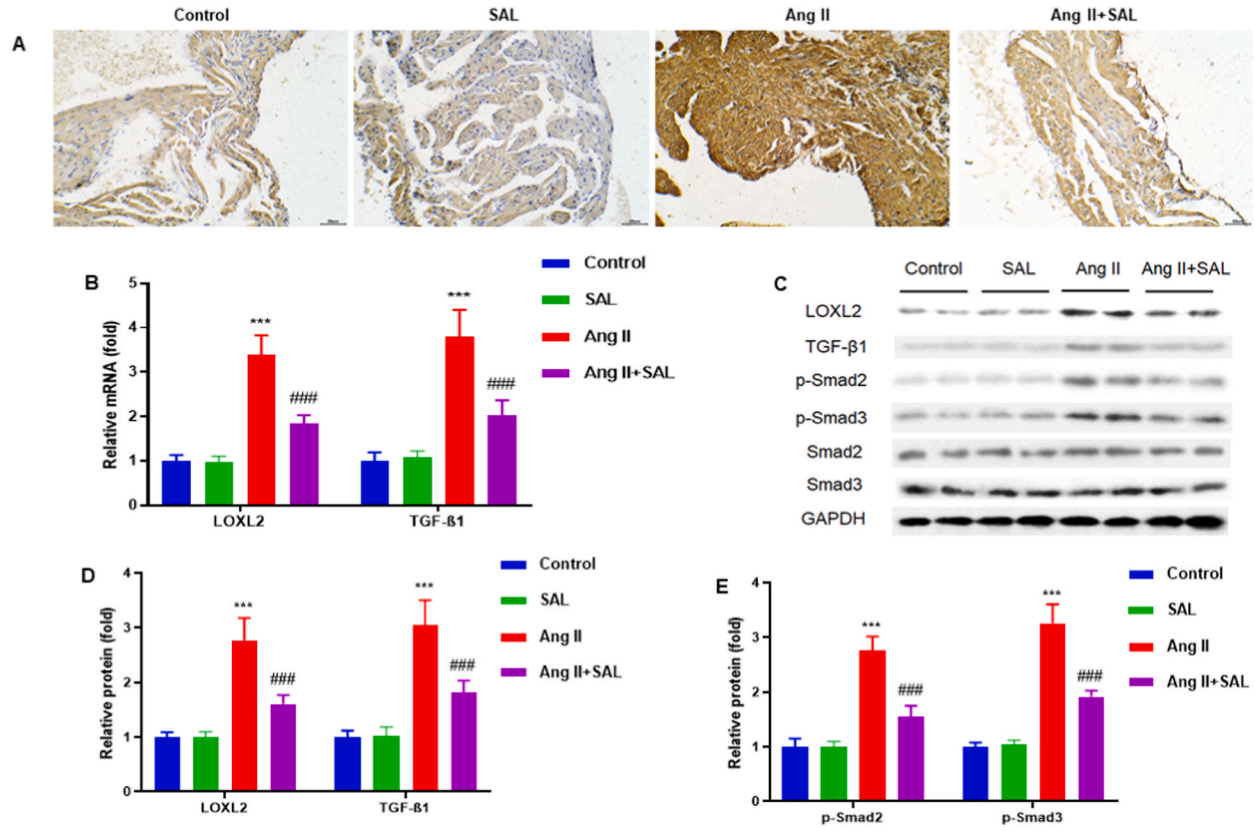

Fig. 5. SAL suppressed the expression of LOXL2 and key factors of the TGF-β1/Smad pathway in Ang II-treated mice. (A) Representative images of LOXL2 by immunohistochemistry. (B) The mRNA expression of LOXL2 and TGF-β1. GAPDH as an internal control. Experiments were run in triplicate. (C) The protein expression was measured by Western blot, and the representative bands are shown. (D) LOXL2 and TGF-β1, (E) *p*-Smad2 and *p*-Smad3 proteins are increased by Ang II and reduced by SAL. LOXL2 and TGF-β1 protein expressions were normalized by GAPDH, *p*-Smad2 protein by Smad2, and *p*-Smad3 protein by Smad3. Data are presented as mean ± SD (n = 8 in each group). ***P < 0.001 vs. control group; ###P < 0.001 vs. Ang II group.

LOXL2 (Fig. 5A). SAL therapy significantly decreased the protein expression of LOXL2, TGF-β1, *p*-Smad2 and *p*-Smad3 in mice compared with Ang II infusion alone (Fig. 5D and E). Therefore, SAL potentially attenuated the expressions of LOXL2 and TGF-β1/Smad pathway proteins in the AF mice model.

5. Limitations

Our research has several limitations. 1) The principles of AF are challenging to understand in clinical studies. However, the primary objectives of the present research were to determine how SAL influenced atrial fibrosis and subsequent AF. 2) We did not assess the dose-dependent impact of SAL on Ang II-infused atrial remodeling. In our further study, we will evaluate a dose-dependent curve analysis to find whether a possible inhibitory effect of SAL was dose-dependent. 3) Even though SAL can attenuate fibrosis, it might not be possible to inhibit it if it already exists. 4) Eight (8) mice were used in each group, and all electrophysiological experiments were performed, which could have an impact on the subsequent pathological examination and protein detection data. Future research should further investigate and verify the subsequent pathological and protein detection data. However, confirming if SAL provides the best impact for patients with chronic AF who also have extensive atrial fibrosis is essential.

6. Conclusion

In recent years, many scientists have conducted in-depth research on treating atrial fibrosis and AF [34–37]. However, there is currently no effective medication to prevent atrial fibrosis. SAL could be a potential therapy to fill up this unmet treatment need. According to the results of the present investigation, SAL effectively decreases Ang II-infused atrial fibrosis and subsequent susceptibility to AF by inhibiting the LOXL2-TGF-1-Smad2/3 pathway (Fig. 6).

Funding statement

This study was supported by (1) Shanghai Pudong New Area Health System Discipline Leader Training Program Project (PWRd2020-20). (2) Pudong New Area Health Committee peak discipline construction (PWYgf2021-04). (3) Key sub specialty of Pudong New Area Health Committee (PWZy2020-08). (4) Key discipline group of Pudong New Area Health and Health Commission (PWZxq2022-11). (5) Epidemiological investigation of atrial fibrillation in Pudong New Area and prospective cohort study on the whole process management of atrial fibrillation under the mode of graded diagnosis and treatment (PKJ2021-Y33).

Data availability statement

Due to confidential issues, the datasets generated and/or analyzed during the current work are not publicly available but are available from the corresponding author upon reasonable request.

Ethics approval and consent to participate

This study was approved by Shanghai Pudong New Area Zhoupu Hospital (Zhoupu Hospital affiliated to Shanghai Medical College of Health) Ethics Committee. The authors envisaged all standard protocols in accordance with the 1964 Declaration of Helsinki. All methods carried out in this study were in accordance with ARRIVE guidelines.

CRediT authorship contribution statement

Zhen Hai: and. **Yingbiao Wu:** Conceived and designed the experiments, Performed the experiments, Analyzed and interpreted the data, Wrote the paper. **Zhongping Ning:** Contributed reagents, materials, analysis tools, or data.

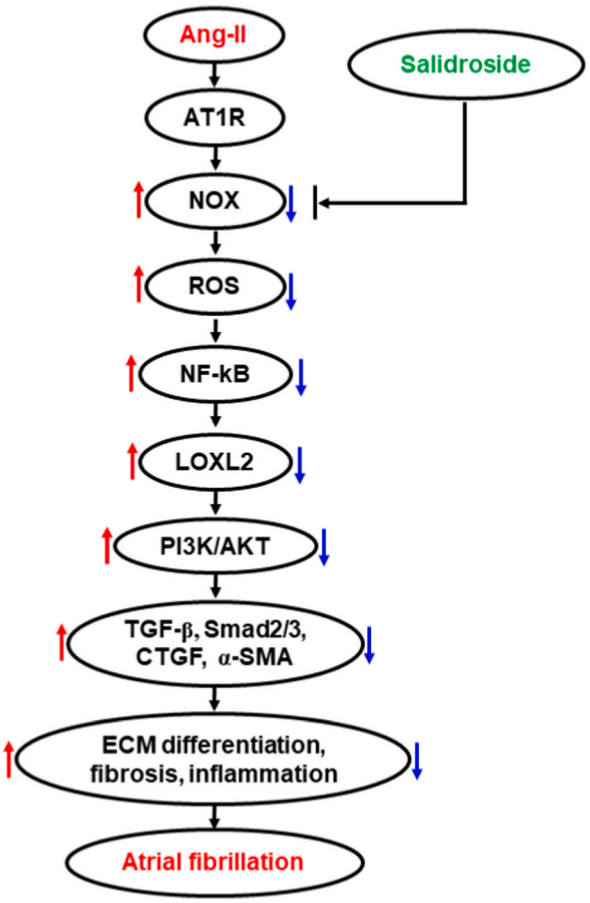

Fig. 6. Model illustration on SAL-mediated protection on Ang II-induced AF (denoted inhibition and indicated stimulation).

Declaration of Competing interest

The authors declared no conflict of interest with other people or organizations.

Acknowledgements

Not applicable.

References

[1] M.S. Dzeshka, G.Y. Lip, V. Snezhitskiy, E. Shantsila, Cardiac fibrosis in patients with atrial fibrillation: mechanisms and clinical implications, J. Am. Coll. Cardiol. 66 (2015) 943–959.
[2] A. Khaji, P.R. Kowey, Update on atrial fibrillation, Trends Cardiovasc. Med. 27 (2017) 14–25.
[3] S. Nattel, Molecular and cellular mechanisms of atrial fibrosis in atrial fibrillation, JACC. Clin. Electrophysiol. 3 (2017) 425–435.
[4] D.R. Van Wagoner, Paracrine signals modulate atrial epicardial progenitor cells and development of subepicardial adiposity and fibrosis implications for atrial fibrillation, Circ. Res. 126 (2020) 1343–1345.
[5] A. Weiss, L. Attisano, The TGFbeta Superfamily Signaling Pathway, vol. 2, Wiley Interdiscip Rev Dev Biol., 2013, pp. 47–63.
[6] Q. Wang, Y. Yu, P. Zhang, Y. Chen, C. Li, J. Chen, et al., The crucial role of activin A/ALK4 pathway in the pathogenesis of Ang-II-induced atrial fibrosis and vulnerability to atrial fibrillation, Basic Res. Cardiol. 112 (2017) 47.
[7] Y. Liu, H. Lv, R. Tan, X. An, X.H. Niu, Y.J. Liu, et al., Platelets promote Ang II (angiotensin II)-induced atrial fibrillation by releasing TGF-β1 (transforming growth factor-β1) and interacting with fibroblasts, Hypertension 76 (2020) 1856–1867.
[8] J. Li, S. Wang, Y.L. Zhang, J. Bai, Q.Y. Lin, R.S. Liu, et al., Immunoproteasome subunit β5i promotes Ang II (angiotensin II)-induced atrial fibrillation by targeting ATRAP (Ang II type I receptor-associated protein) degradation in mice, Hypertension 73 (2019) 92–101.
[9] A. Millanes-Romero, N. Herranz, V. Perrera, A. Iturbide, J. Loubat-casanovas, J. Gil, et al., Regulation of heterochromatin transcription by Snail 1/LOXL2 during epithelial-to-mesenchymal transition, Mol cell 52 (2013) 746–757.
[10] S.D. Vallet, S. Ricard-Blum, Lysyl oxidases: from enzyme activity to extracellular matrix cross-links, Essays Biochem. 63 (2019) 349–364.
[11] J. Yang, K. Savvatis, J.S. Kang, P. Fan, H. Zhong, K. Schwartz, et al., Targeting LOXL2 for cardiac interstitial fibrosis and heart failure treatment, Nat. Commun. 7 (2016), 13710.
[12] Y. Zhao, K. Tang, X. Tianbao, J. Wang, J. Yang, D. Li, Increased serum lysyl oxidase-like 2 levels correlate with the degree of left atrial fibrosis in patients with atrial fibrillation, Biosci. Rep. 37 (2017), BSR20171332.
[13] X.L. Bai, X.L. Deng, G.J. Wu, W.J. Li, S. Jin, Rhodiola and salidroside in the treatment of metabolic disorders, Mini Rev. Med. Chem. 19 (2019) 1611–1626.
[14] F. Xu, J. Xu, X. Xiong, Y. Deng, Salidroside inhibits MAPK, NF-κB, and STAT3 pathways in psoriasis-associated oxidative stress via SIRT1 activation, Redox Rep. 24 (2019) 70–74.
[15] B. Song, G. Huang, Y. Xiong, J. Liu, L. Xu, Z. Wang, et al., Inhibitory effects of salidroside on nitric oxide and prostaglandin E2 production in lipopolysaccharide-stimulated RAW 264.7 macrophages, J. Med. Food 16 (2013) 997–1003.
[16] Y. Zhang, Y. Yao, H. Wang, Y. Guo, H. Zhang, L. Chen, Effects of salidroside on glioma formation and growth inhibition together with improvement of tumor microenvironment, Chin. J. Cancer Res. 25 (2013) 520–526.
[17] Y. Zhu, Y.P. Shi, D. Wu, Y.J. Ji, X. Wang, H.L. Chen, et al., Salidroside protects against hydrogen peroxide-induced injury in cardiac H9c2 cells via PI3K-Akt dependent pathway, DNA Cell Biol. 30 (2011) 809–819.
[18] S. Guan, Y. Xiong, B. Song, Y. Song, D. Wang, X. Chu, et al., Protective effects of salidroside from Rhodiola rosea on LPS-induced acute lung injury in mice, Immunopharmacol. Immunotoxicol. 34 (2012) 667–672.
[19] R. Lu, Y. Wu, H. Guo, X. Huang, Salidroside protects lipopolysaccharide-induced acute lung injury in mice, Dose Response 14 (2016), 1559325816678492.
[20] K.C. Lan, S.C. Chao, H.Y. Wu, C.L. Chiang, C.C. Wang, S.H. Liu, et al., Salidroside ameliorates sepsis-induced acute lung injury and mortality via downregulating NF-κB and HMGB1 pathways through the upregulation of SIRT1, Sci. Rep. 7 (2017), 12026.
[21] Y.L. Zhang, H.J. Cao, X. Han, F. Teng, C. Chen, J. Yang, et al., Chemokine receptor CXCR-2 initiates atrial fibrillation by triggering monocyte mobilization in mice, Hypertension 76 (2020) 381–392.
[22] L. Li, X. Hou, R. Xu, C. Liu, M. Tu, Research review on the pharmacological effects astragaloside IV, Fundam, Clin. Pharmacol. 31 (2017) 17–36.
[23] J.Y. Ma, W.X. Zhang, H. Chen, Y. Jiang, P.F. Tu, H. Ding, The protective effects of echinacoside on oxidative stress injury in vascular dementia rats, Chin. Pharmacol. Bull. 30 (2014) 638–642.
[24] S. Nattel, M. Harada, Atrial remodeling and atrial fibrillation: recent advances and translational perspectives, J. Am. Coll. Cardiol. 63 (2014) 2335–2345.
[25] D. Opacic, K.A. van Bragt, H.M. Nasrallah, U. Schotten, S. Verheule, Atrial metabolism and tissue perfusion as determinants of electrical and structural remodelling in atrial fibrillation, Cardiovasc. Res. 109 (2016) 527–541.
[26] N.L. Rosin, A. Falkenham, M.J. Sopel, T.D. Lee, J.F. Légaré, Regulation and role of connective tissue growth factor in AngII-induced myocardial fibrosis, Am. J. Pathol. 182 (2013) 714–726.
[27] Y. Tsubakihara, A. Moustakas, Epithelial-mesenchymal transition and metastasis under the control of transforming growth factor β, Int. J. Mol. Sci. 19 (2018) 3672.
[28] Y. Yue, K. Meng, Y. Pu, X. Zhang, Transforming growth factor beta (TGF-β) mediates cardiac fibrosis and induces diabetic cardiomyopathy, Diabetes Res. Clin. Pract. 133 (2017) 124–130.
[29] J. Heger, R. Schulz, G. Euler, Molecular switches under TGFβ signaling during progression from cardiac hypertrophy to heart failure, Br. J. Pharmacol. 173 (2016) 3–14.
[30] T. Chen, J. Li, J. Liu, N. Li, S. Wang, H. Liu, et al., Activation of SIRT3 by resveratrol ameliorates cardiac fibrosis and improves cardiac function via the TGF-β/Smad3 pathway, Am. J. Physiol. Heart Circ. Physiol. 308 (2015) 424–434.
[31] J. Lu, J. Shi, M. Li, B. Gui, R. Fu, G. Yao, et al., Activation of AMPK by metformin inhibits TGF-β-induced collagen production in mouse renal fibroblasts, Life Sci. 127 (2015) 59–65.
[32] X. Wen, Y. Liu, Y. Bai, M. Li, Q. Fu, Y. Zheng, LOXL2, a copper-dependent monoamine oxidase, activates lung fibroblasts through the TGF-β/Smad pathway, Int. J. Mol. Med. 42 (2018) 3530–3541.
[33] O.G. de Jong, L.M. van der Waals, F.R.W. Kools, M.C. Verhaar, B.M.W. van Balkom, Lysyl oxidase-like 2 is a regulator of angiogenesis through modulation of endothelial-to-mesenchymal transition, J. Cell. Physiol. 234 (2019) 10260–10269.
[34] O. Adam, C. Zimmer, N. Hanke, R.W. Hartmann, B. Klemmer, M. Böhm, et al., Inhibition of aldosterone synthase (CYP11B2) by torasemide prevents atrial fibrosis and atrial fibrillation in mice, J. Mol. Cell. Cardiol. 85 (2015) 140–150.
[35] X.Q. Chen, X. Liu, Q.X. Wang, M.J. Zhang, M. Guo, F. Liu, et al., Pioglitazone inhibits angiotensin II-induced atrial fibroblasts proliferation via NF-kb/TGF-b1/TRIF/TRAF6 pathway, Exp. Cell Res. 330 (2015) 43–55.
[36] B. Henry, B. Gabris, Q. Li, B. Martin, M. Giannini, A. Parikh, et al., Relaxin suppresses atrial fibrillation in 24 month old rats by reversing atrial fibrosis and upregulating sodium channels, J. Am. Coll. Cardiol. 65 (2015) A380.
[37] J. Jalife, K. Kaur, Atrial remodeling, fibrosis, and atrial fibrillation, Trends Cardiovas. Med. 25 (2015) 475–484.